ISBN: 978-3-95450-192-2 doi:10.18429/JACoW-IBIC2017-TUPCF11

UPGRADE OF THE BEAM POSITION MONITORING SYSTEM AT THE J-PARC MAIN RING FOR HIGH INTENSITY OPERATION *

Aine Kobayashi†, Takeshi Toyama, Kenichiro Satou, Hironori Kuboki,
High Energy Accelerator Research Organization (KEK),
J-PARC Center, Tokai-mura, Naka, Ibaraki, Japan

Abstract

For the T2K neutrino oscillation experiment an upgrade programs of J-PARC are on-going for higher beam intensity. The goal of 10-year upgrade plan is to achieve a beam power of 1.3 MW in the main ring [1], a significant increase compared to the presently achieved power of 470 kW. Beam loss causes the limitation on the proton bunch intensity. A precise orbit correction is necessary in order to reduce the beam loss. Beam position monitor (BPM) is a vital element providing accurate measurements of the beam positions for the control of closed orbit distortion (COD). The current position resolution is a few 10 μm in the COD mode, a few 100 μm in the turn-by-turn mode [2], and the goal is make one tenth of it. Currently an apparent dependence of RMS of COD on the beam intensity is observed (about 100 ~ 200 μm). In order to understand the nature of the phenomenon, investigations are being made on the BPM response and its intensity dependence as well as on the effects of wake field, local orbit bumps to COD and septum. Status of the studies will be discussed.

PROCESSING CIRCUIT FOR THE MR BPMS

The BPM of the MR is a diagonal cut which is nondestructive to the beam, readout from both horizontal and vertical electrodes as shown in Fig. 1. The number of BPM is 186, placed around the MR. After signal processing with Fourier transformation, the position of the beam is defined. The calibration such as beam based alignment (BBA) and beam based gain calibration (BBGC) are implemented [3].

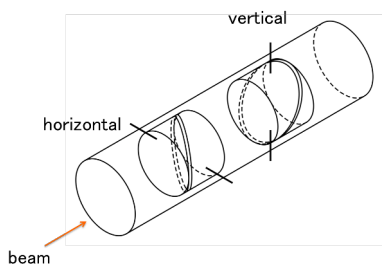

Figure 1: The schematic view of the MR BPM.

COD WITH INTENSITY DEPENDENCE

There are 9 RF buckets in the MR and up to 8 bunches can be filled. The kickers [4] inject bunches every 40 ms at K1, K2, K3 and K4 timing. After 10 ms of the K4 timing, acceleration is started. Usually, the RMS of COD is not dependent on the number of bunches. But an apparent dependence on the beam intensity is observed [5]. When the beam intensity exceeds about 10^{14} ppp, the RMS of COD is observed to grow by 100 ~ 200 μm as shown in Fig. 2.

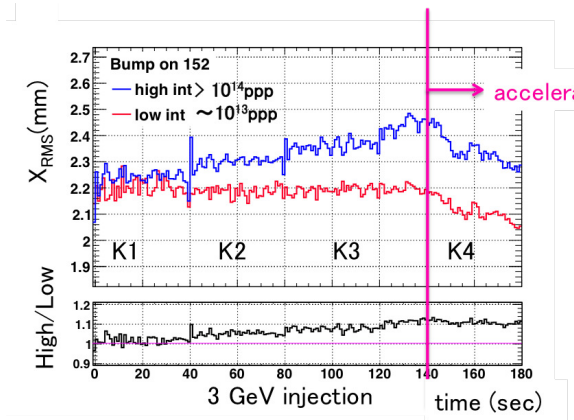

Figure 2: COD excursion of high intensity (> 10^{14} ppp) compared to low intensity (~ 10^{13} ppp) with bump on QFR152.

MEASUREMENTS

Referring to the study which investigated the COD made by a transverse impedance of a local bump in VEPP-4M accelerator, Russia [6], a measurement menu was contained with changing the local bump as well as changing a beam intensity. The fast extraction (FX) kicker and the septum are chosen as the position of the local bump. The size of bumps were arranged with the aperture and not to exceed beam loss about 10^{12} ppp. The taken sets with high beam intensity ($> 2.4 \times 10^{14}$ ppp) are: without bump, with a bump on QFR152 with 10 mm for the FX kicker, with a bump on QFR152 with 4 mm for the septum, and with bumps on both QFR152 (10 mm) and QFR82 (4 mm). Also, the data of low beam intensity (~ 6.0×10^{13} ppp) with a bump on QFR152 wih 10 mm. About 10 to 20 shots were taken for each sets. The MR power was 470 kW at most, with 3 GeV extraction. The number of bunches was up to 8.

BPM RESPONSE

It is necessary to examine BPM signals that are processed to the COD. The typical signals of high intensity beam are shown in Fig. 3, the number of counts from horizontal (upper) and vertical (bottom) electrodes. This measurement

* Work supported by JSPS-JP16H06288
† aine.kobayashi@kek.jp

ISBN: 978-3-95450-192-2 doi:10.18429/JACoW-IBIC2017-TUPCF11

was done with 2 bunches, and the counts (up to 3000) are lower than the maximum $2^{13} \sim 8000$, where the BPM has linearity. Figure 4 shows the peak-to-peak of signals as a function of all the BPM, around the MR. The details of the monitor systems are described in references such as [7]. The above statement that the intensity dependent COD increment does not come from some particular BPMs malfunction, was also confirmed with the result of Fourier transform of the COD (increment), in which the peak is at 21st harmonic of one MR revolution, closest integer to the horizontal tune.

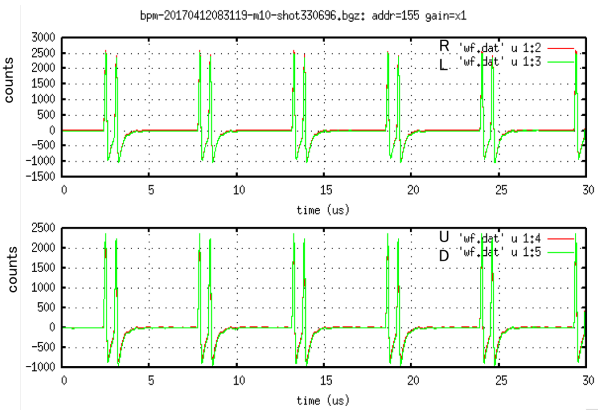

Figure 3: A typical BPM response at high intensity.

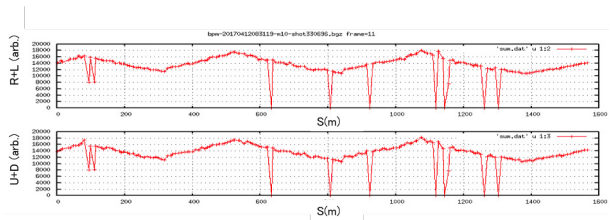

Figure 4: All the BPM counts. The discontinuity of the counts, corresponding to BPM # 13 and 15 has a special amp for some test, and the other with count zero are masked BPM. The detail of the monitor system is described in the reference [7].

COD DATA ANALYSIS

COD Data Correction

The measured COD contains the contribution from ripple noise ($\Delta B/B$) and momentum dispersion ($\eta_s \Delta p/p$), which have to be removed before the analysis [8]. The MR bending magnets are divided into 6 families for connecting power supplies. The dispersion function can be defined by fitting with each of 6 families. The measured COD ($x_{\mathrm{measured}}(s)$) is given as Eq. (1).

$$x_{\mathrm{measured}}(s) = x_{\mathrm{COD}}(s) + \sum_{k=1}^{6} \lambda_k \eta_k(s) \qquad (1)$$

Here, η_k is a dispersion function of a k^{th} family, and an unknown quantity λ_k is defined by fitting to the data. Using the twiss parameters given by the optics calculation, fitting function can be made as shown in Fig. 5. The results by fitting and then subtracted are shown in Fig. 6 and 7.

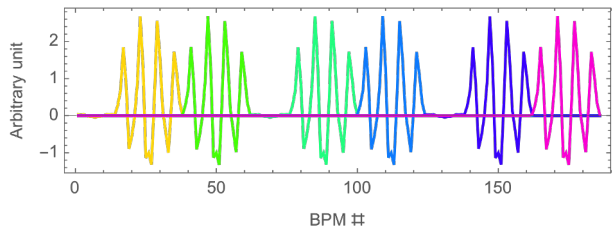

Figure 5: Momentum dispersion function from optical calculation.

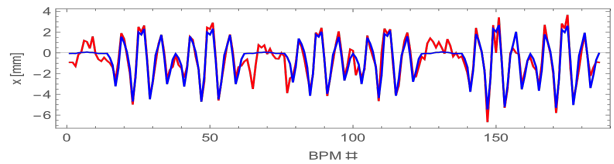

Figure 6: Fit with dispersion function. The red line is the measured value and the blue line is fitting result.

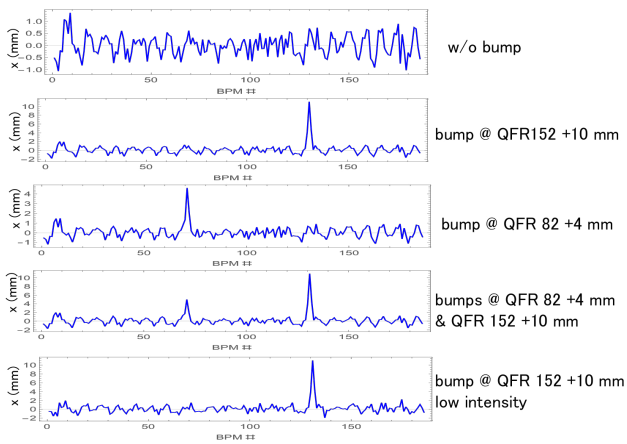

Figure 7: Dispersion effects subtracted from COD of each data-sets. QFR82 and QFR152 corresponding to BPM#71 and 131.

Error Source Search

The error source, which causes the COD excursion was searched by optics calculation tool, SAD [9]. The way of optics correction with small number of magnets by chi-square is described in a paper such as [10]. The COD $x(s_j)$ is measured as Eq. (2) with transport matrix and error source $\theta(s_i)$.

$$x(s_j) = \sum_{i=1} \frac{\sqrt{\beta(s_j)\beta(s_i)}}{2\sin(\pi\nu)} \cos(\pi\nu - |\psi(s_i) - \psi(s_j)|)\theta(s_i) \qquad (2)$$

The COD correction algorithm derives the $\theta(s_i)$ of each given source. In this study, Micado which is implemented

ISBN: 978-3-95450-192-2 doi:10.18429/JACoW-IBIC2017-TUPCF11

in SAD a kind of chi-square cod correction was applied. The candidates of the error source were given 93 steering magnets ZSH, 13 kicker magnets KM, 14 magnetic septa MS, and 2 slow magnet septa SMS.

In order to compare the difference in intensity, the same local bump but different intensity sets were used. The Fig. 8 (top) shows the averaged COD at K4 timing <K4> in high intensity which is large COD and that of K1 intensity <K1> at K1 timing which is small COD. As expected, the position having a local bump was indicated as an error sources when using the COD subtracted <K1> from <K4> as shown in Fig. 8 (bottom). Searching the error sources, Fig. 9 was obtained. Applying Micado to find the largest ten error sources in the given candidates, Fig. 10 (top) was obtained. Then simulated COD with single kicks corresponding the ten error sources is shown in Fig. 10 (bottom).

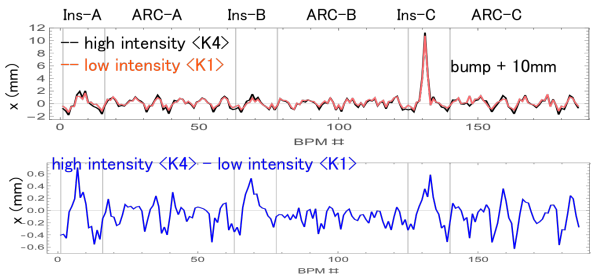

Figure 8: The COD with bump on QFR152 (BPM131) with high and low intensity (top), their difference is the bottom.

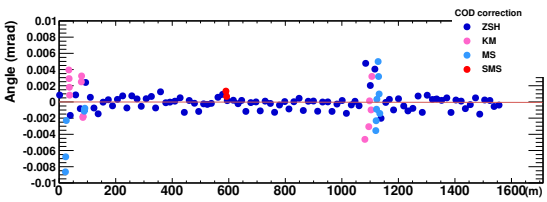

Figure 9: Correction from each sources for COD subtracted <K1> of low intensity from <K4> of high intensity.

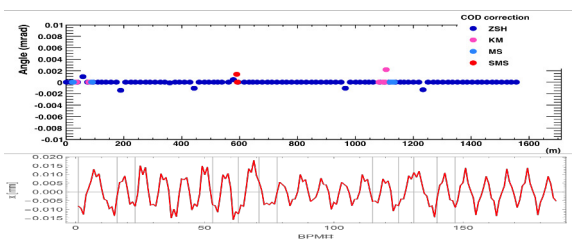

Figure 10: The largest ten error sources in the given candidates (top) and that of simulated COD (bottom).

In the same way, as shown in Fig. 11, the error source search using the COD with or without a local bump were performed. These results also indicates the position of the local bump. Note that the aperture of the septum at QFR82 is small, no more than 4 mm local bump could be made.

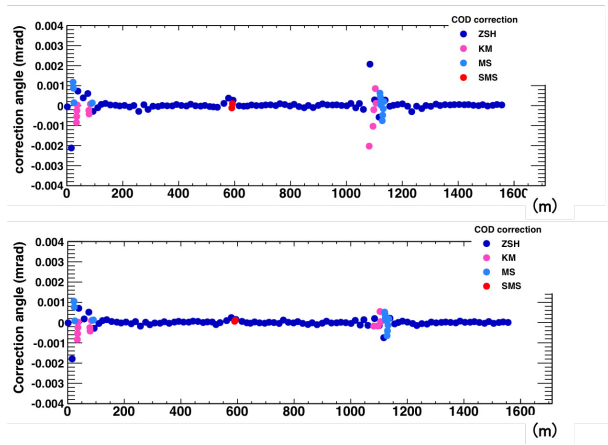

Figure 11: The error source of COD, subtracted the COD of <K4-K1> without bump from the COD <K4-K1> with bump on QFR152 (top) and QFR82 (bottom).

WAKE FIELD ESTIMATION

The most suspected near QFR152 is the FX kicker. Therefore, a wake field caused by a beam when passing through the FX kicker with a local bump was calculated using CST PARTICLE STUDIO [11]. The kicker was modeled as Figs. 12 and 13 referring to [12, 13]. The beam was set to away from center by 10 mm, and the integral path for wake field calculation was set to go along the center. A wake potential and a wake impedance were given as shown in Fig. 14, 15 and 16. The result is close to the previous stretched-wire measurement [14]. The kick factor can be given as Eq. (3) [15].

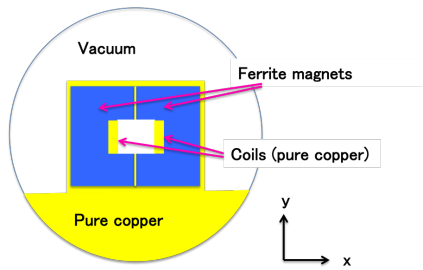

Figure 12: The schematic view of the simplified FX kicker cross-section. The kicker is made of ferrite magnets, pure copper coils and plates, and resistive elements, putting into a vacuum duct.

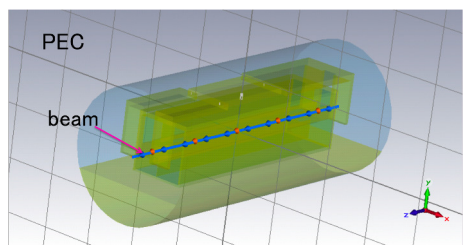

Figure 13: The simplified FX kicker model for a wake field estimation. The appropriate boundary conditions and a simplified resistive circuit [12, 13] were applied.

ISBN: 978-3-95450-192-2 doi:10.18429/JACoW-IBIC2017-TUPCF11

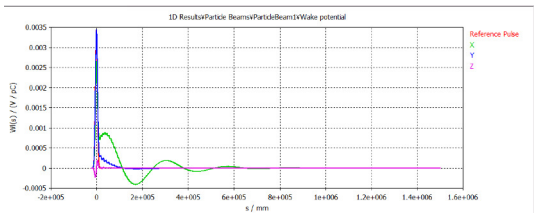

Figure 14: Wake potential.

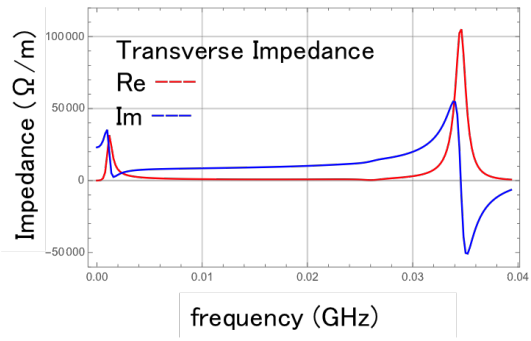

Figure 15: Transverse wake coupling impedance of real part (red) and imaginary part (blue), applied FFT with a roll-off factor 0.2.

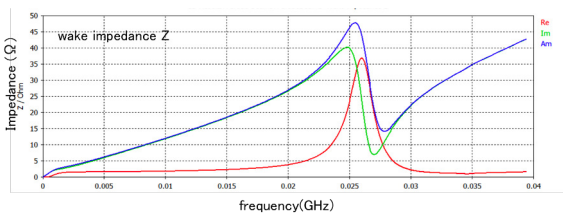

Figure 16: Wake coupling impedance of Z. The results is consists of the previous measurement [14].

$$\kappa_\perp = \frac{1}{\pi}\int_0^\infty d\omega Im\left(Z_\perp(\omega)\right)h(\omega), \tag{3}$$

where $Z_\perp$ is the transverse impedance, ω is the frequency and h is the bunch power spectrum. Then, the kick angle with 10 mm local bump on the kicker per one bunch can be estimated as 0.001 mrad from Eq. (4).

$$\Delta\theta = \frac{q}{(B\rho)c}\kappa_\perp \Delta x, \tag{4}$$

where q is the bunch charge, and $B\rho$ is the magnetic rigidity, c is the speed of light and Δx is the transverse offset of the bunch. The result is in the same order with SAD calculation as shown in a previous section. Nevertheless precise agreement remains for further investigation.

CONCLUSION

For upgrade of MR beam intensity, it is necessary to make clear to what causes the COD excursion. Using the optics simulation and the electromagnetic simulator, the effects from wake field at a local bump were studied. The obtained kick angle was almost consist with a previous measurement.

The correlation between COD and betatron tune shift need to be carefully examined. A tune shift measurement was performed with single bunch in 2×10^{13} ppp beam intensity on 2015 [16]. The measurement with 8 bunch in high intensity is planned in the near future.

A study for both development and improvement of the BPM are also planning for high intensity beam operation.

ACKNOWLEDGEMENT

This study was supported by MR staff members. Special thanks to S. Igarashi, Y. Sato and N. Yamamoto for instruction of SAD and useful suggestions, and J. Takano for operating bumping orbit. This work was supported by JSPS Grant-in-Aid for Specially Promoted Research Grant Number JP16H06288.

REFERENCES

[1] Y. Sato, “MR upgrade”, presented at ATAC2017, J-PARC, 2017.

[2] T. Toyama *et al.*,“Repair and improvement of the J-PARC MR BPM”, in *Proc. PASJ’10*, paper SUP075, 2010.

[3] M. Tejima *et al.*,“Beam based calibration for beam position monitors”, in *Proc. IBIC’2015*, paper TUBLA01, 2015.

[4] T. Sugimoto *et al.*,“Performance of Injection Kicker Magnet for the J-PARC Main Ring”, in *Proc. PASJ’9*, paper THLR08, 2009.

[5] S. Igarashi, 2017 March, private communication, J-PARC.

[6] V. Kiselev and V. Smaluk, “Measurement of local impedance by an orbit bump method”, NIM A 525(2004) 433-438.

[7] S. Hatakeyama *et al.*,“A system for monitoring of the transverse injection error and betatron tune in J-PARC MR”, in *Proc. PASJ’7*, paper WEPS098, 2007.

[8] T. Toyama *et al.*, “Beam-based Alignment of the BPMs at J-PARC MR”, in *Proc. PASJ’11*, paper SAP088, 2011.

[9] SAD homepage. `http://acc-physics.kek.jp/SAD/index.html`

[10] B. Autin and Y. Marti, “Closed orbit correction of A.G. machines using a small number of magnets”, CERN ISR-MA/73-17 (1973).

[11] CST - Computer Simulation Technology homepage. `https://www.cst.com/products/cstps`

[12] Specifications of the FX-kicker magnet and circuit, from K. Ishii.

[13] K. Koseki *et al.*, “Status of the Fast Extraction Kicker of the J-PARC-MR”, presented at ATAC2010, J-PARC, 2010.

[14] T. Toyama *et al.*, “Instability: Observation and Study Results of MR”, presented at ATAC2011, J-PARC, 2011.

[15] B. W. Zotter and S. A. Kheifets, “Ipmpedances and Wakes in High-Energy Particle Accelerators”, ISBN: 9789810226268.

[16] T. Toyama *et al.*, “Impedance and Instabilities”, presented at ATAC2016, J-PARC, 2016.